

PROPERTIES OF THE W BOSON

L. TAYLOR

*Department of Physics, Northeastern University,
Boston, MA 02115, USA*

The properties of the W boson are reviewed. Particular emphasis is placed on recent measurements from the LEP2 and Tevatron experiments.

1 Introduction

The W boson was discovered^{1,2} by the UA1 and UA2 experiments at the CERN Sp \bar{p} S collider in 1983. Since then, its properties have been measured by UA1 and UA2, by the CDF³ and D $\bar{0}$ ⁴ experiments at the FNAL Tevatron, and more recently by ALEPH,⁵ DELPHI,⁶ L3,⁷ and OPAL⁸ at the LEP e⁺e⁻ collider at CERN. In this paper we describe the production and decays of W's (Sec. 2); the determination of the W width (Sec. 3); constraints on anomalous couplings of the W (Sec. 4); and measurements of the W mass (Sec. 5).

2 W Production and Decay

2.1 W Production and Decay at LEP

W-pairs are produced at LEP II through Z/ γ s-channel and neutrino t-channel processes⁹ (the so-called CC03 processes), as shown in Fig. 1(upper). Other diagrams, such as those shown in Fig. 1(lower) lead to the same final states and interfere with the CC03 processes. The identification of W-pairs at LEP II is more difficult than that of Z's at LEP I due to the considerable amount of Standard Model background. At $\sqrt{s} = 161$ GeV (~ 10 pb⁻¹/experiment) the backgrounds are approximately two orders of magnitude more than the signals. At $\sqrt{s} = 172$ GeV (~ 10 pb⁻¹/experiment) the situation is about five times better due to the increasing W-pair cross-section.

The main background to the channel WW \rightarrow q \bar{q} q \bar{q} (γ) comes from the e⁺e⁻ \rightarrow q \bar{q} (γ) process which has a cross-section of approximately 150 pb. Signal events are selected by requiring the events to have high multiplicities and low missing energy. Radiative Z return events are rejected. The WW \rightarrow q \bar{q} $\ell\nu$ (γ)

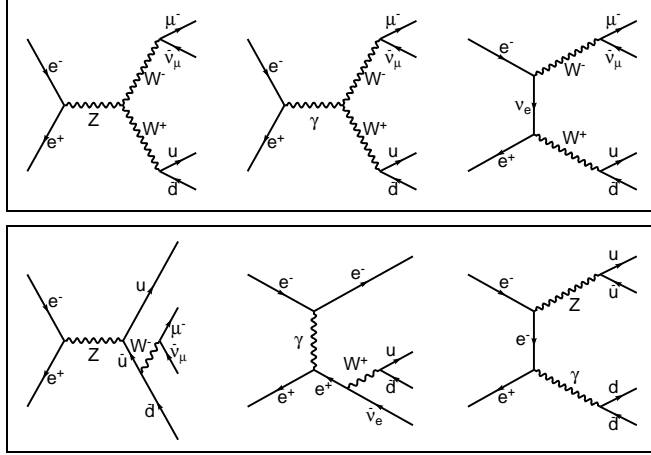


Figure 1: Upper: The CC03 diagrams for W-pair production in e^+e^- collisions with, in this example, subsequent decays to $q\bar{q}$ and $\mu\nu$. Lower: Three important four-fermion diagrams which interfere with the CC03 processes.

samples are selected by requiring the event to have two high energy jets and an isolated charged lepton. The neutrino momentum is inferred from the missing energy. The main backgrounds come from mis-identified $e^+e^- \rightarrow q\bar{q}(\gamma)$ events and from the four-fermion process $e^+e^- \rightarrow q\bar{q}\ell^+\ell^-$ in which one of the leptons is undetected. The $WW \rightarrow \ell\nu\ell\nu(\gamma)$ samples are obtained by requiring the presence of two charged leptons and by excluding high multiplicity (hadronic) events. The dominant backgrounds are from the radiative-return $Z \rightarrow \ell^+\ell^-$, Bhabha, and two-photon processes.

Tab. 1 shows typical values for W-pair selection efficiencies at LEP and the resulting event sample sizes at $\sqrt{s} = 161$ GeV and $\sqrt{s} = 172$ GeV. After correcting for the measured luminosity, the detector acceptances, reconstruction efficiencies, and backgrounds the experiments have fitted their data to extract the LEP average results:^{10–15} $\text{Br}(W \rightarrow e\nu) = (12.0 \pm 1.9)\%$, $\text{Br}(W \rightarrow \mu\nu) = (10.3 \pm 1.7)\%$, $\text{Br}(W \rightarrow \tau\nu) = (10.7 \pm 2.2)\%$, where the errors are dominated by the statistical uncertainties. Assuming lepton universality yields^{10–15} $\text{Br}(W \rightarrow \ell\nu) = (11.0 \pm 0.7)\%$ ($\ell = e/\mu/\tau$) and $\text{Br}(W \rightarrow q\bar{q}') = (67.0 \pm 2.1)\%$, in agreement with the Standard Model predictions of $\text{Br}(W \rightarrow \ell\nu)_{\text{SM}} = 10.83\%$ and $\text{Br}(W \rightarrow q\bar{q}')_{\text{SM}} = 67.5\%$. Assuming $\text{Br}(W \rightarrow \ell\nu)_{\text{SM}}$, the cross-sections (for CC03 processes) are determined to be $\sigma_{\text{WW}}(161\text{GeV}) = (3.67 \pm 0.42)$ pb and $\sigma_{\text{WW}}(172\text{GeV}) = (11.95 \pm 0.70)$ pb. The W mass-dependence of the cross-section close to threshold is used to determine the W mass, as described in

section 5.1.

2.2 *W Production and Decay at the Tevatron*

The production of W 's in $p\bar{p}$ collisions at the Tevatron, which occurs predominantly through quark-antiquark annihilation, is described elsewhere in these proceedings.¹⁶ For both CDF and $D\theta$, candidate W events are triggered by a single lepton trigger and are then required to contain a charged lepton with transverse momentum of typically $p_T^\ell > 25$ GeV and missing energy of typically $\cancel{E}_T > 25$ GeV. Efficiencies for selecting leptonic W decays, including the effects of the trigger, geometric acceptance, and selection and kinematic cuts, are 25–30% for electrons and 5–10% for muons.¹⁷ Typical yields for CDF($D\theta$) are therefore 700(800) $W \rightarrow e\nu$ decays/ pb^{-1} and 150(350) $W \rightarrow \mu\nu$ decays/ pb^{-1} . The corresponding backgrounds are typically 10–20%. These numbers correspond to the pre-selected samples and can change appreciably in the various analyses as more stringent selection criteria are applied.

CDF and $D\theta$ have measured the products of the cross-section and leptonic branching ratio, $\sigma_W \cdot \text{Br}(W \rightarrow \ell\nu)$ and $\sigma_Z \cdot \text{Br}(Z \rightarrow \ell\ell)$, using the background-subtracted number of observed events in each channel, corrected for acceptance, efficiency, and luminosity. Such measurements are a good test of our understanding of QCD and the Parton Distribution Functions (PDF's), for which NLO corrections are 20% and NNLO corrections are about 3%.^{18,19} These calculations predict $\sigma_W = 22.35$ nb and $\sigma_Z = 6.708$ nb, for the CTEQ2M PDF. Using the theoretical expectation of $\text{Br}(W \rightarrow \ell\nu) = (10.84 \pm 0.02)\%$ ²⁰ and the LEP measurement of $\text{Br}(Z \rightarrow \ell^+\ell^-) = (3.366 \pm 0.006)\%$,²¹ yields expectations of $\sigma_W \cdot \text{Br}(W \rightarrow \ell\nu) = (2.42_{-0.11}^{+0.13})$ nb and $\sigma_Z \cdot \text{Br}(Z \rightarrow \ell\ell) = (0.226_{-0.009}^{+0.011})$ nb, where the errors are dominated by the uncertainties in the PDF. Fig. 2 summarises these measurements and demonstrates the good agreement with the theoretical predictions, shown by the shaded band. In future, experiments may

Table 1: Typical values for W -pair selection efficiencies at LEP and the resulting event sample sizes, at $\sqrt{s} = 161$ GeV and $\sqrt{s} = 172$ GeV.

WW event sample	Selection efficiency (%)		Events/experiment	
	$\sqrt{s} = 161$ GeV	$\sqrt{s} = 172$ GeV	$\sqrt{s} = 161$ GeV	$\sqrt{s} = 172$ GeV
$q\bar{q}q\bar{q}(\gamma)$	~ 60	75 – 85	9 – 15	55 – 65
$q\bar{q}\ell\nu(\gamma)$	60 – 80	60 – 90	11 – 16	40 – 50
$\ell\nu\ell\nu(\gamma)$	40 – 70	45 – 80	2 – 6	5 – 10
Total			22 – 36	95 – 120

ultimately use measurements of $\sigma_W \cdot \text{Br}(W \rightarrow \ell\nu)$ to measure their luminosity.

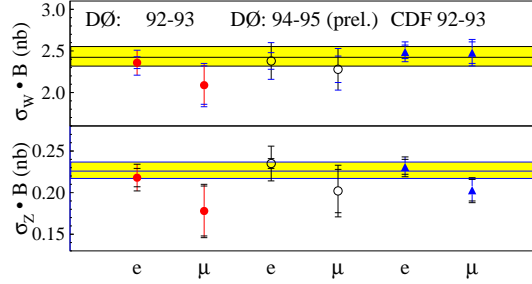


Figure 2: Summary of W and Z cross-section times leptonic branching ratio measurements. The shaded band denotes the theoretical prediction described in the text.

These measurements may alternatively be used to determine $\text{Br}(W \rightarrow \ell\nu) \equiv \Gamma_{\ell\nu}/\Gamma_W$. Experimentally, it is appropriate to measure the ratio R , defined as $R = (\sigma_W \cdot \text{Br}(W \rightarrow \ell\nu)) / (\sigma_Z \cdot \text{Br}(Z \rightarrow \ell\ell))$ since a number systematics uncertainties cancel, including that from the luminosity determination and some of those from the acceptance and efficiency estimations. Fig. 3(left) summarises the measurements of R from the Tevatron and the Sp \bar{p} S experiments.¹⁷ The W leptonic branching ratio is given by $\text{Br}(W \rightarrow \ell\nu) = R \times$

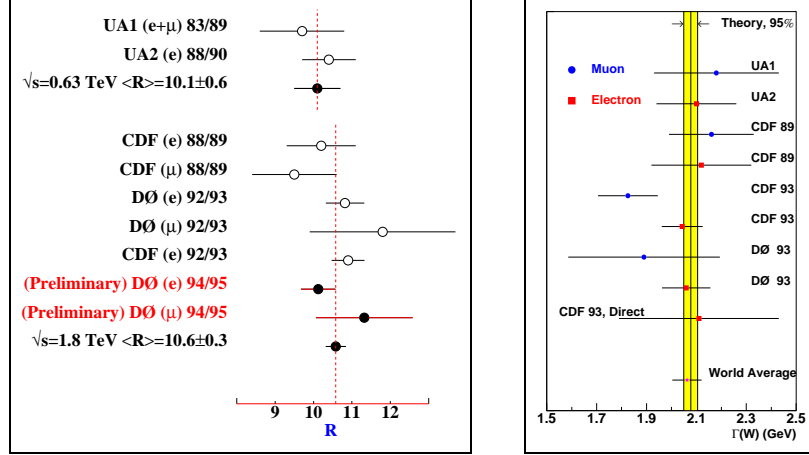


Figure 3: Sp \bar{p} S and Tevatron measurements of the ratio R and of the W width.

$(\sigma_Z/\sigma_W) \times \text{Br}(Z \rightarrow \ell\ell)$ The ratio of cross-sections is taken from the theory^{18,19}

to be $\sigma_W/\sigma_Z = 3.33 \pm 0.03$ at $\sqrt{s} = 1.8$ TeV and $\sigma_W/\sigma_Z = 3.26 \pm 0.09$ at $\sqrt{s} = 0.63$ TeV, again with the advantage that some of the systematic uncertainties cancel. The LEP measurement of $\text{Br}(Z \rightarrow \ell^+\ell^-) = (3.366 \pm 0.006)\%$ ²¹ is used. The results from CDF, $\text{Br}(W \rightarrow \ell\nu) = (10.94 \pm 0.45)\%$,¹⁷ and from DØ, $\text{Br}(W \rightarrow \ell\nu) = (10.43 \pm 0.44)\%$,²² are in good agreement with the preliminary measurements from LEP, the average of which is $\text{Br}(W \rightarrow \ell\nu) = (11.0 \pm 0.7)\%$.¹⁵

3 W Width

Precise measurements of the W width, like those of the Z width, may yield evidence for non-standard decays involving, for example, supersymmetric particles^{23,24} or heavy quarks.²⁵ The ratio R measured by the Tevatron and SpP̄S experiments may be used to determine the W width, $\Gamma_W = (1/R) \times (\sigma_W/\sigma_Z) \times (\Gamma_{\ell\nu}/\text{Br}(Z \rightarrow \ell\ell))$. Taking $\Gamma_{\ell\nu} = (225.2 \pm 1.5)$ MeV from theory,²⁰ σ_W/σ_Z from theory^{18,19} as above, and the LEP²¹ measurement of $\text{Br}(Z \rightarrow \ell^+\ell^-)$ yields the results for Γ_W shown in Fig. 3(right). This figure also shows the less-precise but direct measurement by CDF of Γ_W from an analysis of the W transverse mass distribution, described in section 5.2.

The world average W width of $\Gamma_W = 2.062 \pm 0.059$ GeV,¹⁷ which allows for correlations from the uncertainty in the PDF's, agrees well with the Standard Model prediction of $\Gamma_W = 2.077 \pm 0.014$ GeV.¹⁷ The allowed partial width for non-Standard Model decays is less than 109 MeV at the 95% confidence level.

4 Anomalous Couplings of the W

Triple Gauge Couplings (TGC's) are central to the Standard Model, for example to preserve unitarity for such sets of diagrams such as those shown in Fig 1(upper). These delicate cancellations are sensitive to physics beyond the Standard Model. The generalised Lorentz-invariant WWZ/WW γ vertices have 14 couplings. The experiments adopt a pragmatic approach and consider only g_1^V , κ_V , and λ_V ($V = \gamma, Z$), which are theoretically favoured.⁹ At tree-level, these may be interpreted in terms of the CP conserving quantities: electric charge, $Q_W = eg_1^\gamma$; magnetic dipole moment: $\mu_W = (e/2m_W)(g_1^\gamma + \kappa_\gamma + \lambda_\gamma)$; and electric quadrupole moment: $q_W = -(e/m_W^2)(\kappa_\gamma - \lambda_\gamma)$. There are similar relations, involving also the Weak mixing angle θ_W , for g_1^Z , κ_Z , and λ_Z . The Standard Model predicts: $g_1^\gamma = g_1^Z = 1$ (i.e. $\Delta g_1^V \equiv g_1^V - 1 = 0$), $\kappa_\gamma = \kappa_Z = 1$ (i.e. $\Delta \kappa_V \equiv \kappa_V - 1 = 0$), and $\lambda_\gamma = \lambda_Z = 0$.

4.1 Anomalous Couplings of the W at LEP

Anomalous couplings at LEP2 are probed by analysing the differential cross-sections for W-pair production in terms of the polar angle of the W^- , and the polar and azimuthal angles of the W^\pm decay products in the W^\pm rest frames. Despite the low statistics of the samples, the first TGC results are impressive. For example, an L3 analysis has excluded $g_{ZWW} = 0$ at $> 95\%$ C.L.

Using a complementary method, L3 has measured the cross-section at $\sqrt{s} = 172$ GeV for the single W production²⁶ process, $e^+e^- \rightarrow e\nu_e W$, which is sensitive to $\Delta\kappa_\gamma$ and λ_γ . The measured cross-section, $\sigma = 0.61_{-0.33}^{+0.43} \pm 0.05$ pb is consistent with the Standard Model and therefore the following 95% C.L. limits are set: $-3.6 < \Delta\kappa_\gamma < 1.5$ and $-3.6 < \lambda_\gamma < 3.6$.

The first LEP TGC results are now being finalised for the (later) summer conferences. In particular they will use a common base set of anomalous couplings parameters and include LEP averages allowing for correlations.

4.2 Anomalous Couplings of the W at the Tevatron

The Tevatron analyses necessarily allow for a form-factor dependence of the anomalous couplings: $\Delta\kappa(\hat{s}) = \Delta\kappa/(1 + \hat{s}/\Lambda^2)^2$; and $\lambda(\hat{s}) = \lambda/(1 + \hat{s}/\Lambda^2)^2$; where \hat{s} is the effective centre of mass energy of the process and Λ is the energy scale which is probed for new physics.

The W pair production cross-section is used to constrain the anomalous couplings. For example, CDF has studied the process $p\bar{p} \rightarrow W^+W^- \rightarrow \ell\nu\ell\nu$ using $\int \mathcal{L} = 108\text{pb}^{-1}$. Di-lepton events ($ee/e\mu/\mu\mu$) with \cancel{E}_T are selected with high efficiency and low backgrounds. The $t\bar{t}$ background is reduced by limiting the hadronic (b jet) activity in the event. CDF observes 5 events, with an expected background of 1.2 ± 0.3 events, which corresponds to a cross section of $\sigma(p\bar{p} \rightarrow W^+W^-) = (10.2_{-5.1}^{+6.3} \pm 1.6)$ pb. Since this is in agreement with the Standard Model expectation of $\sigma(p\bar{p} \rightarrow W^+W^-) = (9.5 \pm 1.0)$ pb, they obtain the following constraints, for $\Lambda = 2\text{TeV}$: $-1.0 < \Delta\kappa < 1.3$ (for $\lambda = 0$) and $-0.9 < \lambda < 0.9$ (for $\Delta\kappa = 0$) assuming $\Delta\kappa_\gamma = \Delta\kappa_Z$ and $\lambda_\gamma = \lambda_Z$.

The processes $p\bar{p} \rightarrow WW \rightarrow \text{jet jet } \ell\nu$ and $p\bar{p} \rightarrow WZ \rightarrow \text{jet jet } \ell^+\ell^-$ have also been analysed, with the advantage that they have higher statistics than the $WW \rightarrow \ell\nu\ell\nu$ analyses. The leptonic W decays are tagged by a high p_T charged lepton and \cancel{E}_T , the hadronic decays by two jets with an invariant mass consistent with m_W , and the Z decays by two charged leptons with an invariant mass consistent with m_Z . The large background from W/Z + jets is reduced by requiring the W to have high p_T . The sensitivity to SM WW/WZ production is thereby sacrificed but not the sensitivity to anomalous processes which tend to populate the high p_T^W region. For $\Lambda = 2\text{TeV}$, CDF obtains: $-0.5 < \Delta\kappa < 0.6$

(for $\lambda = 0$) and $-0.4 < \lambda < 0.3$ (for $\Delta\kappa = 0$) assuming $\Delta\kappa_\gamma = \Delta\kappa_Z$ and $\lambda_\gamma = \lambda_Z$. In this analysis, $D\emptyset$ enhances the sensitivity by fitting the lepton spectrum but, since only the Run 1a data is used, less stringent constraints are obtained.

The radiation of photons from W 's is also sensitive to anomalous couplings. For example, $D\emptyset$ uses their standard W sample and requires in addition a high transverse energy photon ($E_T^\gamma > 10$ GeV). The large background from initial/final state radiation from fermions is suppressed by requiring the photon to be well isolated. From a fit to the E_T^γ spectrum $D\emptyset$ obtains, for $\Lambda = 1.5$ TeV: $-1.0 < \Delta\kappa < 1.0$ (for $\lambda = 0$) and $-0.3 < \lambda < 0.3$ (for $\Delta\kappa = 0$) assuming $\Delta\kappa_\gamma = \Delta\kappa_Z$ and $\lambda_\gamma = \lambda_Z$.

5 W Mass

At LEP there are two complementary methods for determining the W mass: from measurements of the W -pair production cross-section close to threshold and from the direct reconstruction of the decay products of the W 's. The Tevatron experiments use their high statistics W samples to perform W mass measurements by direct reconstruction.

5.1 W Mass from LEP

Fig. 4(left) shows the variation of the W -pair production cross-section (CC03 processes) in e^+e^- collisions in the threshold region for various values of the W mass as predicted in the context of the Standard Model by the GENTLE²⁷ program. For the threshold method the optimum sensitivity to m_W is at $\sqrt{s} \approx 2m_W + 0.5$ GeV, hence the choice of $\sqrt{s} = 161.33 \pm 0.05$ GeV for the initial phase of LEP running in 1996. Fig. 4(right) shows the predicted cross-section as a function of m_W , for $\sqrt{s} = 161.33$ GeV. Using the measurement, $\sigma_{WW}(161\text{GeV}) = (3.67 \pm 0.42)$ pb the LEP average for m_W is determined to be¹⁴ $m_W = 80.40 \pm 0.22$ GeV. Allowance is made for common systematic errors (0.07 GeV) which include only a small contribution (0.03 GeV) from the uncertainty in the LEP centre-of-mass energy. The individual LEP measurements are shown in Fig. 5.

At $\sqrt{s} = 172$ GeV the W mass is determined by reconstruction of the W decay products using the channels $W^+W^- \rightarrow q\bar{q}q\bar{q}$ and $W^+W^- \rightarrow q\bar{q}\ell\nu$ ($\ell = e, \mu, \tau$).²⁸ For the $W^+W^- \rightarrow q\bar{q}q\bar{q}$ channel, selected events are forced to contain four jets. The two correct pairs of jets yield two measurements of the W mass for each event. There are a number of ways of kinematically reconstructing the W mass for a given event: using the ‘‘raw’’ reconstructed jet

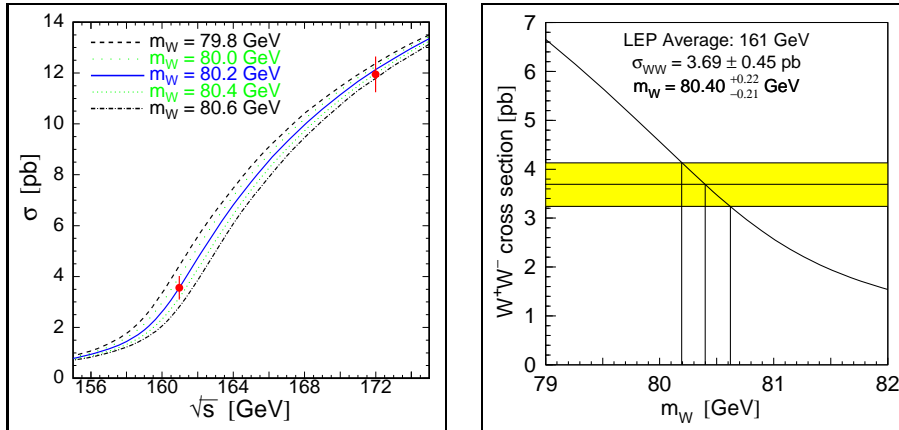


Figure 4: Left: Variation of the W -pair production cross-section in e^+e^- collisions in the threshold region for various values of the W mass (as predicted by the GENTLE program). The data points, which corresponds to the LEP average cross-sections, illustrate the sensitivity of a threshold cross-section measurement to the W mass. Right: The determination of the W mass from the variation of the predicted cross-section (at $\sqrt{s} = 161.33 \pm 0.05$ GeV) as a function of the W mass.

pairs; scaling the jet energies such that each pair of jets has the beam energy; performing a 4-C fit by enforcing energy and momentum conservation on the whole event; performing a 5-C fit where the two measured W masses are forced to be equal. Typically, the scaling of the jet energies gives a large improvement while the additional gains of the 4-C and 5-C fits are more modest. There are three possible pairings of jets, only one of which corresponds to the two W decays. Typically the pair with the highest kinematic fit probability is retained although some analyses also use the second pairing if it has a sufficiently high probability. Fig. 6 shows the results of the OPAL W mass analysis of the $W^+W^- \rightarrow q\bar{q}q\bar{q}$ channel for (a) the best fit pairing (60 events expected and 67 observed), and (b) the second best fit pairing (17 events expected and 17 observed).

The $W^+W^- \rightarrow q\bar{q}\ell\nu$ analyses force the selected events to contain two jets. The charged lepton is reconstructed with high precision and efficiency using standard techniques developed at LEP 1, while the neutrino kinematics are inferred from the missing energy in the event. This channel has no combinatorics and less background than the four-jet channel. However, since reconstruction of the neutrino “uses up” three degrees of freedom, only 1-C or 2-C fits may be used for the extraction of the W mass. Fig. 6 shows the results of the OPAL

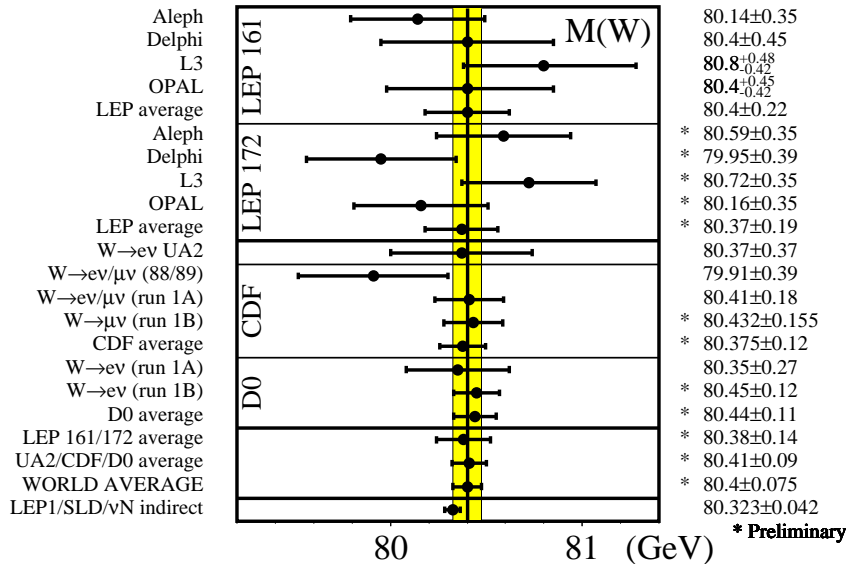


Figure 5: Summary of W mass measurements.

W mass analysis for (c) $W^+W^- \rightarrow q\bar{q}(e/\mu)\nu$ (31 events seen for 33 expected) and (d) $W^+W^- \rightarrow q\bar{q}\tau\nu$ (16 events seen for 12 expected).

The W mass is obtained from the data assuming that the invariant mass distribution is described by a relativistic Breit-Wigner convoluted with an experimental resolution function and a phase-space function to account for the fit constraints. Biases from the following sources are also taken into account: initial state radiation, the event selection efficiencies, the mass reconstruction, and the fitting method. These are generally determined from Monte Carlo studies of the differences in the true and fitted W masses and applied to the value of m_W obtained from the data. In the L3 analysis, such effects are implicitly included through the use of many Monte Carlo samples (with differing input W masses) which are used to construct the likelihood distribution for the data as a function of m_W .

Fig. 5 summarises the W mass measurements^{14, 28} from ALEPH, DELPHI, L3, and OPAL using the data at $\sqrt{s} = 172$ GeV. The systematic errors on m_W , using OPAL as an example,²⁸ include: detector effects (64 MeV); hadronisation (44 MeV); fit procedure (43 MeV); initial state radiation (27 MeV); colour recombination and Bose-Einstein correlations (50 MeV); LEP beam en-

OPAL Preliminary

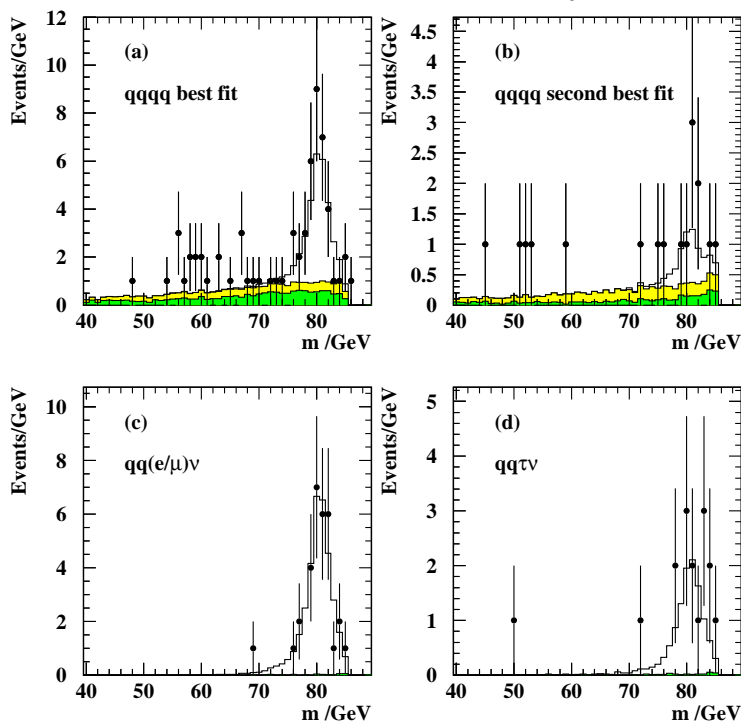


Figure 6: Reconstructed invariant mass spectra from the OPAL W^+W^- analysis at $\sqrt{s} = 172$ GeV for (a) best-fit jet-pairing in $W^+W^- \rightarrow q\bar{q}q\bar{q}$ events; (b) second-best-fit jet-pairing in $W^+W^- \rightarrow q\bar{q}q\bar{q}$ events; (c) $W^+W^- \rightarrow q\bar{q}\ell\nu$ ($\ell = e, \mu$), and (d) $W^+W^- \rightarrow q\bar{q}\tau\nu$. The data are shown as points with error bars. The open histogram denotes the total Monte Carlo expectation normalised to the integrated luminosity, the light histogram denotes combinatorial background, and the dark histogram denotes other backgrounds.

ergy uncertainty (30 MeV). The latter two are completely correlated between experiments and are taken into account when deriving the average LEP 172 value¹⁴ of $m_W = 80.37 \pm 0.19$ GeV. Many of these systematic errors will be reduced as more data are collected and analysed although future reductions in the uncertainty from the colour recombination and Bose-Einstein correlations will require theoretical as well as experimental input.

The average of all the LEP threshold and the direct reconstruction measurements is $m_W = 80.38 \pm 0.14$ GeV, where allowance has been made for

common systematic errors.¹⁴

5.2 *W Mass from the Tevatron*

The CDF W mass measurements are based on 24 pb^{-1} of $W \rightarrow (e/\mu)\nu$ data from 1988/89^{29,30} and Run 1a^{31,32} and, more significantly, on $\sim 90 \text{ pb}^{-1}$ of $W \rightarrow \mu\nu$ data from Run 1b.^{33,34} $D\theta$ W mass measurements are based on $W \rightarrow e\nu$ data from Run 1a³⁵ ($\sim 15 \text{ pb}^{-1}$) and Run 1b^{22,36} ($\sim 80 \text{ pb}^{-1}$).

W mass measurements from the Tevatron (see review of M. Demarteau¹⁷ for more details) are based on fits to distributions of transverse mass, $m_T = \sqrt{2p_T^\ell p_T^\nu (1 - \cos \phi^{\ell\nu})}$, where: p_T^ℓ and p_T^ν denote the transverse momenta of the charged lepton (e or μ) and the neutrino respectively, and $\phi^{\ell\nu}$ denotes the angle between the charged lepton and the neutrino in the transverse plane. The value of p_T^ν is inferred from the measured missing energy, allowing for the luminosity-dependent transverse energy flow of the underlying minimum-bias interactions. The transverse mass is preferred to the transverse momentum of the charged lepton because to first order it is independent of the modelling of the transverse momentum of the W . On the other hand, it relies on the precise and accurate determination of p_T^ν which is a challenging experimental task.

For the W mass measurement it is crucial to understand the energy scale and resolution of the charge lepton measurements. CDF determines the muon momentum scale using measurements of the J/ψ invariant mass. The extrapolation from the J/ψ to the higher average momenta of $W \rightarrow \mu\nu$ decays, allowing for possible non-linearities, is cross-checked using measurements of the Υ and Z invariant masses. The uncertainty on the muon momentum scale results in a 40 MeV uncertainty on the W mass measurement. $D\theta$ has performed a similar study to determine the electron energy scale, using the measured invariant mass spectra for $\pi^0 \rightarrow \gamma\gamma$, $J/\psi \rightarrow e^+e^-$, and $Z \rightarrow e^+e^-$ decays. Possible non-linear effects are constrained using test-beam data. The charged lepton energy resolutions are verified using the $Z \rightarrow \ell^+\ell^-$ samples.

The W mass is determined from the measured m_T distributions by comparison with Monte Carlo distributions with differing input W masses. The Monte Carlo programs generate the W 's as a relativistic Breit-Wigner resonance with a longitudinal momentum distribution according to various PDF models (MRSA', MRSD', CTEQ2M, and CTEQ3M). The modelling of the W transverse momentum, the underlying event, and multiple interactions is determined and/or checked using W , Z , and minimum-bias data samples. Background contributions, which are at the few percent level, include $Z \rightarrow \ell^+\ell^+$ decays in which one of the leptons is lost, $W \rightarrow \tau\nu$; $\tau \rightarrow \ell\nu\nu$ decays, and mis-identified QCD di-jet events. Fig. 7(upper left) shows the m_T distributions for the back-

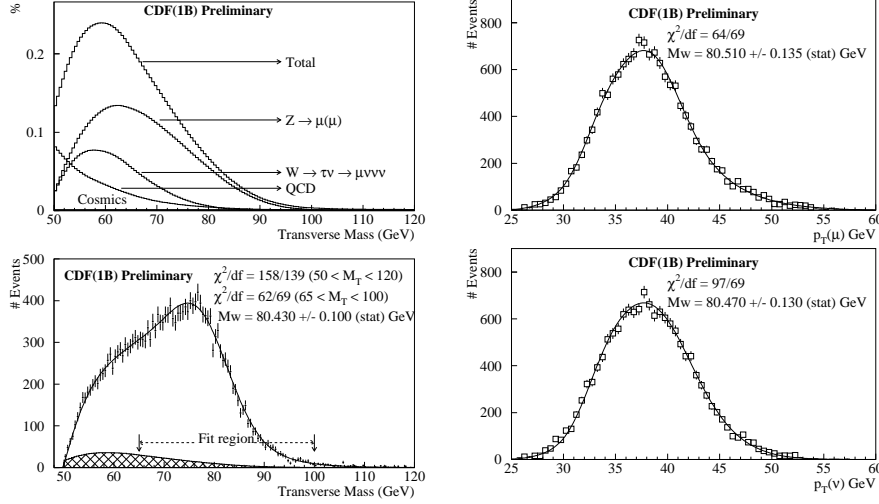


Figure 7: Distribution of transverse mass, m_T , from the CDF run 1b $W \rightarrow \mu\nu$ analysis, for background (upper left) and the data (lower left), showing the result of the fit for m_W (solid line) and the estimated background contribution (hatched). Distributions of muon (upper right) and neutrino (lower right) transverse momenta from the CDF run 1b $W \rightarrow \mu\nu$ analysis, with the results of the fits for m_W .

ground contributions to the CDF Run 1b $W \rightarrow \mu\nu$ analysis. Fig. 7(lower left) shows the $W \rightarrow \mu\nu$ data of CDF together with the result of the fit. The uncertainties on the CDF W mass from this analysis,³⁴ which are typical of the Tevatron analyses, include the following sources: statistics (100 MeV); momentum scale (40 MeV); momentum resolution (25 MeV); PDF's (25 MeV); QED (20 MeV); QCD (20 MeV); input p_T of the W 's (40 MeV); recoil model (90 MeV); trigger bias (15 MeV); selection bias (10 MeV); background (25 MeV); and fitting systematics (10 MeV). As a cross-check, both CDF and $D0$ also fit the charged lepton and neutrino p_T distributions to extract the W mass. They obtain results which are consistent with the m_T fit results, as shown in Fig. 7(right) for CDF.

The average CDF W mass, allowing for a common error of 60 MeV for all their measurements, is $m_W = 80.375 \pm 0.120$ GeV.³⁴ After inclusion of the electron channel, CDF anticipates that the final W mass error from the Run 1 data will be $\sigma(m_W) \approx 100$ MeV³³. The average $D0$ W mass is $m_W = 80.44 \pm 0.11$ GeV.³⁶ $D0$ anticipates that their final Run 1 W mass analysis, including the end cap region ($1.5 < |\eta_e| < 2.5$), will yield a W mass error of

Table 2: Indirect and direct determinations of m_W , m_t , and m_H .

	m_W (GeV)	m_t (GeV)	m_H (GeV)
LEP1/SLC/ νN (indirect)	80.323 ± 0.042	155^{+10}_{-9}	36^{+52}_{-18}
LEP2/Tevatron (direct)	80.400 ± 0.075	175.6 ± 5.5	> 77 (unofficial)
Combined fit	80.366 ± 0.031	172.7 ± 5.4	127^{+127}_{-72}

$\sigma(m_W) \approx 100$ MeV.²² Fig. 5 summarises the W mass measurements from CDF and D \emptyset . The UA2 result also shown is determined from their measurement of the ratio $m_W/m_Z = 0.8813 \pm 0.0036 \pm 0.0019$ ³⁷, which is scaled to the LEP value of $m_Z = 91.187 \pm 0.007$ GeV.²¹ The hadron collider average is $m_W = 80.41 \pm 0.09$ GeV, where a common error of 65 MeV has been assumed.³⁴

5.3 Interpretation of W Mass Measurements

Fig. 5 summarises the W mass measurements from ALEPH, DELPHI, L3, OPAL, UA2, CDF, and D \emptyset . The average of these direct measurements is $m_W = 80.400 \pm 0.075$ GeV. This is in good agreement with the indirect prediction from a fit to electroweak measurements³⁸ (m_Z , A_{FB} , A_{LR} , etc.) of the LEP1, SLC, and νN scattering³⁹ experiments, which yields $m_W = 80.323 \pm 0.042$ GeV.¹⁴ The fit also results in predictions for the top and Higgs masses, as shown in table 2. The indirect determination of m_t is in agreement with the direct measurement of CDF/D \emptyset of $m_t = 175.6 \pm 5.5$ GeV.⁴⁰

Loop corrections give rise to a quadratic dependence of m_W on m_t and a logarithmic dependence of m_W on m_H , as shown schematically in Fig. 8(left). Fig. 8(right) illustrates the variation of m_W with m_t for various values of m_H , shown as bands. The data point denotes the direct measurements of m_W from LEP and the Tevatron and of m_t from the Tevatron. The LEP/SLC/ νN contour for the indirect determination is consistent with the direct measurements.

A combined fit, in the context of the Standard Model, to the indirect electroweak measurements and the direct measurements of m_W and m_t yields $m_W = 80.366 \pm 0.031$ GeV, $m_t = 172.7 \pm 5.4$ GeV and $m_H = 127^{+127}_{-72}$ GeV. The apparently high significance of the low value of m_H should be interpreted with caution; the likelihood is approximately parabolic in $\log m_H$, therefore the upper bound is less constrained than it would appear to be from the quoted 1σ error. The upper limit on the Higgs mass at the 95% confidence level is $m_H < 465$ GeV, indicating that the data weakly favour a low mass Higgs.

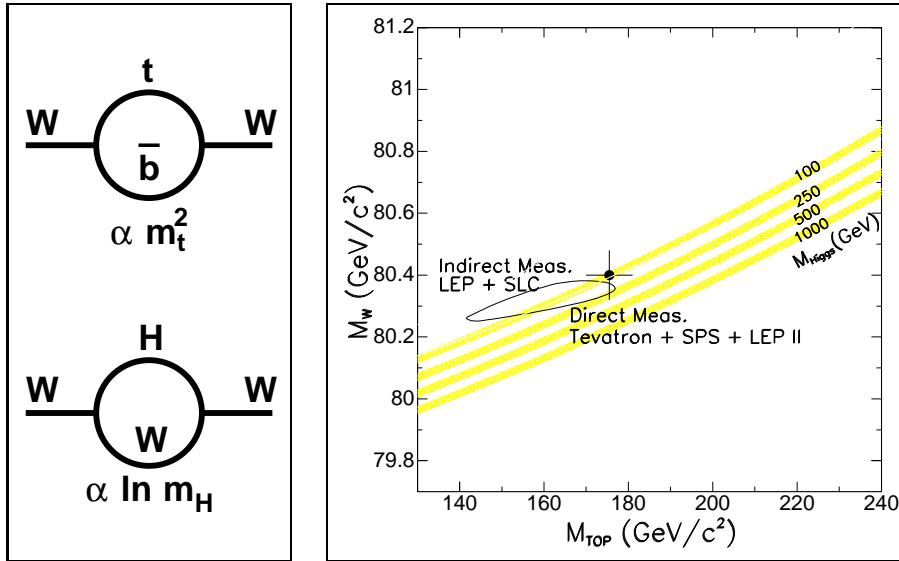


Figure 8: Left: Loop corrections giving rise to a dependence of m_W on m_t and m_H . Right: The variation of m_W with m_t for various values of m_H , shown as bands, compared to the direct measurements of m_W from LEP and the Tevatron and of m_t from the Tevatron. The LEP/SLC contour for the indirect determination of m_W and m_t is consistent with the direct measurement.

Acknowledgements

I would like to thank all the people who, sometimes unknowingly, greatly facilitated the preparation of this review, in particular: A. Blondel, S. Christen, R. Clare, M. Demarteau, D. Errede, P. Fisher, M. Grünwald, A. Gurtu, J. Mnich, K. Mönig, T. Paul, C. Paus, D. Stickland, N. Watson, and D. Wood. It is a pleasure to acknowledge the hard work of the organisers who made the conference such a success.

1. UA1 Collab., G. Arnison et al.. *Phys. Lett.*, B122:103, 1983.
2. UA2 Collab., M. Banner et al.. *Phys. Lett.*, B122:476, 1983.
3. CDF Collab., F. Abe, et al. *Nucl. Instrum. & Methods.*, A271:387, 1988.
4. D0 Collab., S.Abachi et al., *Nucl. Instr. & Meth.* **A338** (1994) 185;
D0 Collab., H.Aihara et al., *Nucl. Instr. & Meth.* **A325** (1993) 393;
D0 Collab., S.Abachi et al., *Nucl. Instr. & Meth.* **A324** (1993) 53.
5. ALEPH Collab., D.Decamp et al., *Nucl. Instr. & Meth.* **A294** (1990) 121;

- ALEPH Collab., D. Buskulic et al., *Nucl. Instr. & Meth.* **A360** (1995) 481.
6. DELPHI Collab., P. Aarnio et al., *Nucl. Instr. & Meth.* **A303** (1991) 233;
DELPHI Collab., P. Abreu et al., *Nucl. Instr. & Meth.* **A378** (1996) 57.
 7. L3 Collab., B. Adeva et al., *Nucl. Instr. & Meth.* **A 289** (1990) 35;
M. Acciarri et al., *Nucl. Instr. & Meth.* **A 351** (1994) 300;
M. Chemarin et al., *Nucl. Instr. & Meth.* **A 349** (1994) 345;
A. Adam et al., Preprint CERN-PPE/96-097 to be published in
Nucl. Instr. & Meth. ;
I.C. Brock et al., *Nucl. Instr. & Meth.* **A 381** (1996) 236.
 8. OPAL Collab., K. Ahmet et al., *Nucl. Instr. & Meth.* **A305** (1991) 275;
OPAL Collab., P. Allport, et al., *Nucl. Instr. & Meth.* **A324** (1993) 34;
OPAL Collab., P. Allport, et al., *Nucl. Instr. & Meth.* **A346** (1994) 476.
 9. G. Altarelli, T. Sjöstrand and F. Zwirner (eds.). Physics at LEP2.
CERN Yellow Report, 96-01:1, 1996.
 10. ALEPH Collab., R. Barate et al.. Measurement of the W Mass in
 e^+e^- Collisions at Production Threshold. *CERN-PPE*, 97-025, 1997.
Submitted to *Phys. Lett. B*.
 11. DELPHI Collab., P. Abreu et al.. *Phys. Lett.*, B397:158, 1997.
 12. L3 Collab., M. Acciarri et al.. Pair-Production of W Bosons in e^+e^-
Interactions at $\sqrt{s} = 161$ GeV. *CERN-PPE*, 97-014, 1997. Accepted by
Phys. Lett. B.
 13. OPAL Collab., K. Ackerstaff et al.. *Phys. Lett.*, B389:416, 1996.
 14. Private communication with the LEP Collaborations and the LEP/SLD
Electroweak Working Group. See also: <http://www.cern.ch/LEPEWWG/>.
 15. A. Gurtu. W Production and Mass Measurements at LEP II. In *Pro-
ceedings of the 11th Rencontre de la Vallee d'Aoste on Results and Per-
spectives in Particle Physics*, La Thuile, Italy, 2-8 March 1997.
 16. G. Guglielmo, these proceedings.
 17. M. Demarteau. Electroweak Measurements from the Tevatron. In *Pro-
ceedings of the Workshop on New Directions for High Energy Physics
(Snowmass96)*, Snowmass, Colorado, USA, 25 June - 12 July 1996.
Available as a preprint: Fermilab-Conf-96/353 or hep-ex/9611018.
 18. R. Hamberg, W.L. van Neerven and T. Matsuura. *Nucl. Phys.*,
B359:343, 1991.
 19. W.L. van Neerven and E.B. Zijlstra. *Nucl. Phys.*, B382:11, 1992.
 20. T. Takeuchi J.L. Rosner, M.P. Worah. *Phys. Rev.*, D49:1363, 1994.
 21. Particle Data Group, R. M. Barnett et al. *Phys. Rev.*, D54:1, 1996.
 22. D. Wood. Electroweak Physics from D0. In *Proc. of the XXXIInd
Rencontres de Moriond*, Les Arcs, France, 15-22 March 1997.
 23. V. Barger et al. *Phys. Rev.*, D28:2912, 1983.

24. X. Tata M. Drees, C.S. Kim. *Phys. Rev.*, D37:784, 1988.
25. J. Terrón T. Alvarez, A. Leites. *Nucl. Phys.*, B301:1, 1988.
26. L3 Collab., M. Acciarri et al.. Production of Single W Bosons at LEP. *CERN-PPE*, 97-28, 1997. Submitted to *Phys. Lett. B*.
27. D. Bardin, A. Leike, and T. Riemann. *Phys. Lett.*, B344:383, 1995.
28. M. Thomson. W Mass at LEP2 from Direct Reconstruction. In *Proc. of the XXXIInd Rencontres de Moriond*, Les Arcs, France, 15-22 March 1997.
29. CDF Collab., F. Abe et al.. *Phys. Rev. Lett.*, 65:2243, 1990.
30. CDF Collab., F. Abe et al.. *Phys. Rev.*, D43:2070, 1991.
31. CDF Collab., F. Abe et al.. *Phys. Rev. Lett.*, 75:11, 1995.
32. CDF Collab., F. Abe et al.. *Phys. Rev.*, D52:4784, 1995.
33. A. Gordon. M_W Measurement with $W \rightarrow \mu\nu$ Decays at CDF for Run 1b. In *Proc. of the XXXIInd Rencontres de Moriond*, Les Arcs, France, 15-22 March 1997.
34. CDF Collab., D. Errede, private communication.
See also: <http://www-cdf.fnal.gov/physics/ewk/wmass.html>.
35. D0 Collab., S. Abachi et al.. *Phys. Rev. Lett.*, 77:3309, 1996.
36. D0 Collab., D. Wood, private communication.
See also: <http://www-d0.fnal.gov/public/wz/wmass/wmass.html>.
37. J. Alitti et al.. *Phys. Lett.*, B276:365, 1992.
38. P. Clarke, these proceedings.
39. K. S. McFarland et al.. *FNAL-Pub-97*, 001-E, 1997. (to be published).
40. R. Raja. "Top Quark Mass Results from CDF and D0". In *Proceedings of the XXXIInd Rencontres de Moriond*, Gif-sur-Yvette, France, 1997. Editions Frontières.